Journal for Electrochemistry and Plating Technology

JEPT

Edited by: DGO-Fachausschuss Forschung – Hilden / Germany

Corrosion protection of 6061 Al-15 Vol. Pct. $SiC_{(p)}$ composite using a biopolymer-An electrochemical approach

The influence of biopolymer starch as corrosion inhibitor on 6061 Al-15 vol. pct. $SiC_{(p)}$ composite in 0.05M hydrochloric acid was studied by potentiodynamic polarization (PDP) and electrochemical impedance spectroscopy (EIS) technique. The surface morphology was studied using SEM, EDX, AFM and XRD techniques. The results showed that the inhibition efficiency of starch increased with increasing inhibitor concentrations and also with increase in temperatures. Starch acted as a mixed inhibitor and underwent chemical adsorption following Langmuir adsorption isotherm.

Received: 2015-08-21
Received in revised form: 2015-12-16
Accepted: 2015-12-17

Keywords:
6061 Al-15 vol. pct. $SiC_{(p)}$ composite, Starch, HCl medium, PDP, EIS, SEM, EDX, AFM, XRD

Authors:
B. P. Charitha, R. Padmalatha

DOI:
10.12850/ISSN2196-0267.JEPTXXXX

LEUZE VERLAG
seit 1902

Corrosion protection of 6061 Al-15 Vol. Pct. $SiC_{(p)}$ composite using a biopolymer- An electrochemical approach

*B. P. Charitha, R. Padmalatha**

Department of Chemistry, Manipal Institute of Technology, Manipal, INDIA

**Email: padmalatha.rao@manipal.edu*

Keywords: 6061 Al-15 vol. pct. $SiC_{(p)}$ composite, Starch, HCl medium, PDP, EIS, SEM, EDX, AFM, XRD
Paper: Received: 2015-08-21 / Received in revised form: 2015-12-16 / Accepted: 2015-12-17
DOI: 10.12850/ISSN2196-0267.JEPTXXXX

The influence of biopolymer starch as corrosion inhibitor on 6061 Al-15 vol. pct. $SiC_{(p)}$ composite in 0.05M hydrochloric acid was studied by potentiodynamic polarization (PDP) and electrochemical impedance spectroscopy (EIS) technique. The surface morphology was studied using SEM, EDX, AFM and XRD techniques. The results showed that the inhibition efficiency of starch increased with increasing inhibitor concentrations and also with increase in temperatures. Starch acted as a mixed inhibitor and underwent chemical adsorption following Langmuir adsorption isotherm.

1. Introduction

The aluminum alloys due to their low density, high thermal and electrical conductivity, damping capacity and good corrosion resistance property are widely used in various engineering applications [1]. The oxide film formed on their surface protects the metal from undergoing corrosion. But aluminum alloys are not hard enough to wear and abrasion, so their applications become limited. In order to overcome this, aluminum alloys are usually reinforced with nano-structured silicon carbides (SiC) particulates which are referred as aluminum metal matrix composites (AMMC). Due to the reinforcement of SiC, aluminum alloys will become hard enough to wear and abrasion, thus they have been used in various engineering applications such as aviation, automobile, aerospace etc. They also have been used in sporting goods, electronic packaging etc. [2–8]. The main drawback of reinforcement is; it enhances the corrosion rate. Micro-galvanic corrosion of AMMCs is more likely to occur during acid pickling and descaling procedures used in the surface preparation of such composites as the ceramic particles function as efficient cathodic sites and trigger corrosion in the presence of acid or moisture. This can be combated by altering the corrosive environment i.e. by adding corrosion inhibitors [9–11]. Usually chemical compounds are used as corrosion inhibition, but some of them cause hazardous to environment as well as to the human beings, they are non–biodegradable and expensive. Now-a-days the research activities are geared towards cost effective, ecofriendly, biodegradable and non–toxic corrosion inhibitors.

Biopolymers are the class of compounds which has various applications in all the sectors of economy. Biopolymers are used as adhesives, lubricants, adsorbents, soil conductors, drug delivery cosmetics etc. Biopolymers are naturally available cheap, non–toxic and environmentally acceptable and some of them showed to function as effective inhibitors for metal corrosion in different acid medium [12].

Starch, the biopolymer of present investigation is a principle carbohydrate storage product of higher plants containing 20% to 25% amylose and 75 % to 80% amylopectin by weight. It has wide range of applications in food industry, pharmaceuticals, paper making and many other industrial branches.

As a part of our studies with ecofriendly inhibitors [13 – 15] for the corrosion control of aluminum material, in the present investigation we demonstrate the applicability of biopolymer starch for the control of 6061 Al-15 vol. pct. $SiC_{(p)}$ composite corrosion in Hydrochloric acid medium.

2. Experimental

2.1 Material

The experiment was performed by using 6061 Al-15 vol. pct. $SiC_{(p)}$ composite. The composition of the base alloy is given in the table 1.

Tab. 1: The composition of the base metal Al–6061 alloy

Elements	Cu	Mg	Cr	Si	Al
Composition(%wt)	0.25	1.0	0.20	0.60	Balance

2.2 Preparation of test coupon

Surface area of 1 cm^2 cylindrical test coupon of aluminum composite metal sealed with resin material was exposed to HCl medium. It was polished with different grade emery papers. Further polishing was done with disc polisher using levigated alumina to get the mirror surface; the specimen was dried and stored in the desiccators for further studies.

2.3 Preparation of medium

The stock solution of HCl of higher concentration was prepared by using 37% HCl and double distilled water. The standardization of HCl was done with standard NaOH solution by volumetric method. From the standard solution, the required concentration of HCl (0.05M) solution was prepared as and when required.

2.4 Preparation of inhibitor solution

Starch (Merck chemicals) was used as such. Molecular weight of starch was in the range of 110,000–150,000 Dalton. Inhibitor solution was prepared by dissolving starch of required strength in hot distilled water. Starch inhibitor solution used was ranging from 100–800ppm.

2.5 Electrochemical measurements

Corrosion behavior studies of 6061 Al-15 vol. pct. $SiC_{(P)}$ composite was conducted by using electrochemical work station (CH600 D–series US model with CH–instrument with beta software). The electrochemical cell used was a conventional three electrode compartment glass cell with Saturated Calomel Electrode (SCE) as reference electrode and Platinum as auxiliary electrode. 6061 Al-15 vol. pct. $SiC_{(P)}$ composite was used as working electrode. All the potential values were recorded with respect to SCE. Immediately after EIS studies, Potentiodynamic polarization studies were carried out on the same electrode without any further surface treatment.

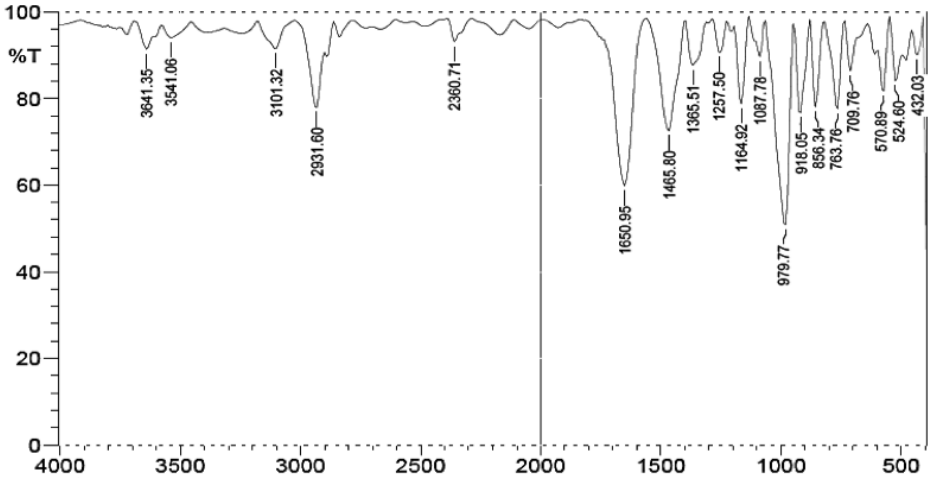

Fig. 1: FTIR spectrum of starch

2.5.1 Potentiodynamic Polarization (PDP) measurement

The Potentiodynamic Polarization studies was carried out for 6061 Al-15 vol. pct. $SiC_{(P)}$ composite material in 0.05M HCl solution separately.

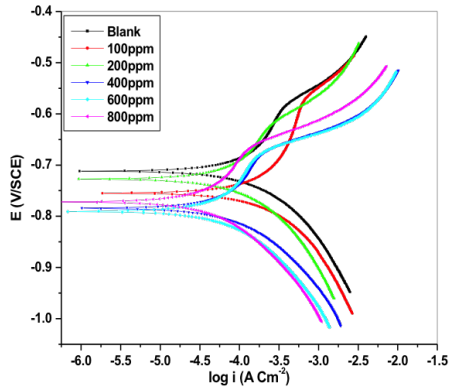

Fig. 2: Potentiodynamic polarization curves for the corrosion of 6061 Al-15 vol. pct. $SiC_{(P)}$ composite in 0.05M HCl containing various [starch] at 35 °C

With reference to SCE the steady states open circuit potential (OCP) was recorded at the end of 1800 seconds. The potentiodynamic current–potential plots are obtained by polarizing the working electrode (W.E) to +250mV anodically and –250mV cathodically with respect to OCP at the scan rate of $1mVsec^{-1}$.

2.5.2 Electrochemical Impedance Spectroscopy (EIS) studies

The EIS measurement for 6061 Al-15 vol. pct. $SiC_{(P)}$ composite material were carried out by using small amplitude of AC signal of 10mV, at the OCP with a frequency ranging from 10000 Hz to 0.01 Hz. In all the above measurements minimum of 3-4 trails were done and average of best three agreeing value was reported.

2.6 Surface studies

In order to carry out the surface analysis; techniques such as SEM, EDX, AFM & XRD were adopted.

2.6.1 Surface Morphology and elemental analysis

Surface Morphology studies of 6061 Al-15 vol. pct. $SiC_{(P)}$ composite was carried out by using analytical scanning electron microscope (JEOL JSM–6380L). Surface morphology of corroded sample was obtained by immersing 6061 Al-15 vol. pct. $SiC_{(P)}$ composite in 0.05M HCl for 2 h and it was compared with uncorroded sample and elemental mapping was done by using Energy Dispersive X–Ray analysis.

2.6.2 Atomic force microscopy

AFM analysis was carried out by using 1B342 innova model. And analysis was done by immersing 6061 Al-15 vol. pct. $SiC_{(P)}$ composite in 0.05M HCl for 2 h and it was compared with uncorroded sample.

2.6.3 X-ray diffraction analysis

XRD analysis was carried out for the scraped product of Al-composite immersed in 0.05M HCl and for the inhibited scraped product using miniflex 600 model.

3. Results and discussion

3.1 Fourier transforms infrared (FTIR) spectroscopy of starch

Figure 1 shows FTIR spectrum of starch. In the fingerprint region between 900 and 1500 cm^{-1}, the absorption bands at 979, 1087, 1164, 1257, 1365, 1465 cm^{-1} corresponds to –C–O–C–, the peak at 1650 cm^{-1} is attributed for tightly bounded H_2O present in starch and the absorption band at 3541 cm^{-1} and 3101 cm^{-1} is attributed for characteristic vibrations of C–H and –OH bonds.

3.2 Electrochemical measurement

3.2.1 Potentiodynamic polarization (PDP) measurement

Anodic and cathodic reaction kinetics occurring on 6061 Al-15 vol. pct. $SiC_{(P)}$ composite in 0.05M HCl solution containing without and with various concentration of starch was studied using Potentiodynamic polarization method. Figure 2. Depicts the Potentiodynamic polarization curve i.e. plot of potential (V) verses corrosion current (i) for 6061 Al-15 vol. pct. $SiC_{(P)}$ composite in 0.05M HCl with various concentration of starch along with blank. Figure 2 reveals the active dissolution of 6061 Al-15 vol. pct. $SiC_{(P)}$ composite in acidic environment. Further examination of Potentiodynamic polarization plots showed small shift in corrosion potential (E_{corr}), this negligible change in the E_{corr} may due to the condition of 6061 Al-15 vol. pct. $SiC_{(P)}$ composite and inhibited reactions of anodic and cathodic area [16]. The shift in both anodic and cathodic slopes towards negative value in comparison with blank indicates that, introduction of starch hindered the corrosion attack on 6061 Al-15 vol. pct. $SiC_{(P)}$ composite in acid medium. It has been also reported that if the shift in E_{corr} exceeds ±85mV in comparison with uninhibited E_{corr} values, the inhibitor behaves either as cathodic or anodic inhibitor. But due to the addition of starch the displacement of E_{corr} is maximum towards +20mV [17] and also cathodic and anodic branches of polarization curves shifted towards lower current density values, thus it can be consider that starch acts as mixed inhibitor.

Various parameters such as E_{corr}, i_{corr} values were obtained by Potentiodynamic polarization studies. By using i_{corr} values percentage inhibition efficiency [I.E(%)] of inhibitor on 6061 Al-15 vol. pct.

$SiC_{(P)}$ composite material corrosion was calculated by using equation (1) [18].

$$I.E\ (\%) = \frac{i_{corr} - i_{corr(inh)}}{i_{corr}} \times 100 \quad (1)$$

Then the corrosion rate in mmy^{-1} was obtained by using the equation (2)

$$CR\ (mmy^{-1}) = \frac{3270 \times M \times i_{corr}}{\rho \times z} \quad (2)$$

where, 3270 is a constant which revels the unit of corrosion rate, ρ is corroding material density (2.66 g cm^{-3}), M is the atomic mass of metal (9.15) , Z is the electrons transferred/ metal atom (3) [19].

Table 2 shown below discloses the Potentiodynamic polarization values for corrosion control of 6061 Al-15 vol. pct. $SiC_{(P)}$ composite in 0.05M HCl. It is observed in the table that there is a shift in $+\beta_a$ values, this shift may be due to adsorption of starch inhibitor molecule over the metal surface. It is also found that I.E(%) of starch increased with increase in concentration of inhibitor and it also found increase with increase in temperature of HCl medium up to maximum value of 95.24% at 50°C at highest concentration 800ppm. This indicates that inhibitor molecule get firmly adsorbed over the metal surface even at very high temperature.

3.2.2 Electrochemical Impedance Spectroscopy (EIS) studies

Nyquist plot of 6061 Al-15 vol. pct. $SiC_{(P)}$ composite for uninhibited and inhibited medium is shown in the figure 3. Semicircle impedance plots were obtained for both uninhibited and inhibited medium. This plot consists of three frequency region, High frequency (HF), Intermediate frequency (IF) and Low frequency (LF) region. Three loops of the impedance plots were assigned to these three frequency regions. That is first capacitive loop at HF region, small inductive loop at IF region and another capacitive loop at LF region. The nyquist plots reported for aluminum corrosion in acidic medium were very well agreed with the obtained nyquist plots [20–27].

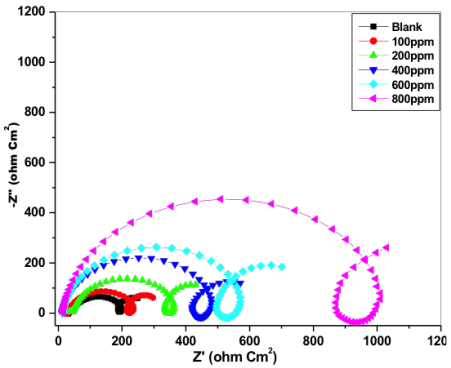

Fig. 3: Impedance plot for corrosion control of 6061 Al-15 vol. pct. $SiC_{(P)}$ composite in 0.05M HCl at 35 °C

6061 Al-15 vol. pct. $SiC_{(P)}$ composite oxidation at M^+/oxide/solution interface corresponds to HF capacitive loop [25–28]. During corrosion process, Al^{+1} get oxidized to Al^{+3}. Through oxide/electrolyte interface Al^{+1} will migrates from M^+/oxide interface and get oxidized to Al^{+3}. At oxide/solution interface OH^- and O^{2-} ions are formed. The capacitive loop at HF region is attributed for the formation of passivating oxide layer on the surface of the metal. The bulk or surface species relaxation in the protective oxide layer leads to inductive loop at IF [29] and it also may be due to the adsorbed inhibitor molecule relaxation over the aluminum surface or due to the incorporation of Cl^- ions, charged intermediates and oxide ions on and into the protective oxide layer. The LF capacitive loop is attributed to dissolution of M^+ ions.

Tab. 2: Results of Potentiodynamic polarization studies for corrosion of 6061 Al-15 vol. pct. $SiC_{(P)}$ composite in 0.05M HCl containing various [starch]

Temp (°C)	[Starch] (ppm)	E_{corr} (mV/ SCE)	i_{corr} (μAcm^{-2})	$+\beta_a$ ($mVdec^{-1}$)	$-\beta_c$ ($mVdec^{-1}$)	CR (mmy^{-1})	I.E (%)
30	Blank	–685	193	105	632	0.73	—
	100	–664	132	125	665	0.48	31.92
	200	–668	120	127	670	0.36	37.93
	400	–668	103	117	632	0.24	46.66
	600	–784	96	55	710	0.21	50.34
	800	–762	54	229	751	0.19	72.07
35	Blank	–755	283	343	601	1.06	—
	100	–712	192	368	648	0.60	32.66
	200	–727	117	562	632	0.48	58.65
	400	–784	95	558	710	0.37	66.07
	600	–791	85	516	681	0.30	69.82
	800	–772	54	631	703	0.22	80.77
40	Blank	–660	412	837	613	1.55	—
	100	–692	131	665	649	0.79	67.81
	200	–673	115	118	672	0.60	71.98
	400	–711	107	811	641	0.48	74.04
	600	–791	85	516	681	0.39	79.29
	800	–782	69	2218	775	0.28	83.07
45	Blank	–746	681	741	636	2.57	—
	100	–689	192	722	639	0.99	71.72
	200	–727	158	562	632	0.76	76.34
	400	–784	96	558	710	0.64	85.89
	600	–773	60	594	711	0.55	91.06
	800	–772	54	631	703	0.42	92.01
50	Blank	–675	803	780	597	3.03	—
	100	–699	225	813	665	1.18	71.81
	200	–661	140	1137	644	0.96	82.80
	400	–788	83	2049	785	0.84	89.55
	600	–782	69	2219	775	0.75	91.30
	800	–763	38	908	701	0.57	95.24

As the concentration of the inhibitor increased, the capacitive loop diameter increased, this indicates the resistance to corrosion attack by the adsorption of inhibitor molecule. Due to the electrode surface inhomogeneity, the semicircle of the impedance plots were depressed [30].

The equivalent circuit consists of nine elements; they are solution resistance (R_S), charge transfer resistance (R_{ct}), Inductive resistance (R_L) and inductive element (L). It also consist of CPE (constant phase element, Q), which is parallel to the series of capacitance C_1 and C_2 and also parallel to the series of resistor R_1, R_2, R_L and R_{ct}. R_L is parallel to L inductor. The circuit with parallel resistor and capacitance were attributed for conduction of ions in oxide layer and to its dielectric constant respectively shown in the figure 4.

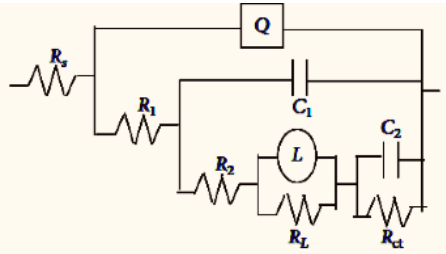

Fig. 4a: Equivalent circuit used to simulate for the obtained impedance values

Double layer capacitance (C_{dl}) and polarization resistance (R_P) can be calculated by using the equations (3) and (4) respectively,

$$C_{dl} = C_1 + C_2 \quad (3)$$

$$R_P = R_1 + R_2 + R_L + R_{ct} \quad (4)$$

For circuit fitment 3.21 version of Zimpwin software was used. Table 3 shows the results obtained from the circuit fitment. The component Q_{dl}, and coefficient 'a' of Q(CPE) quantifies some physical phenomena like inhomogeneous of surface of the

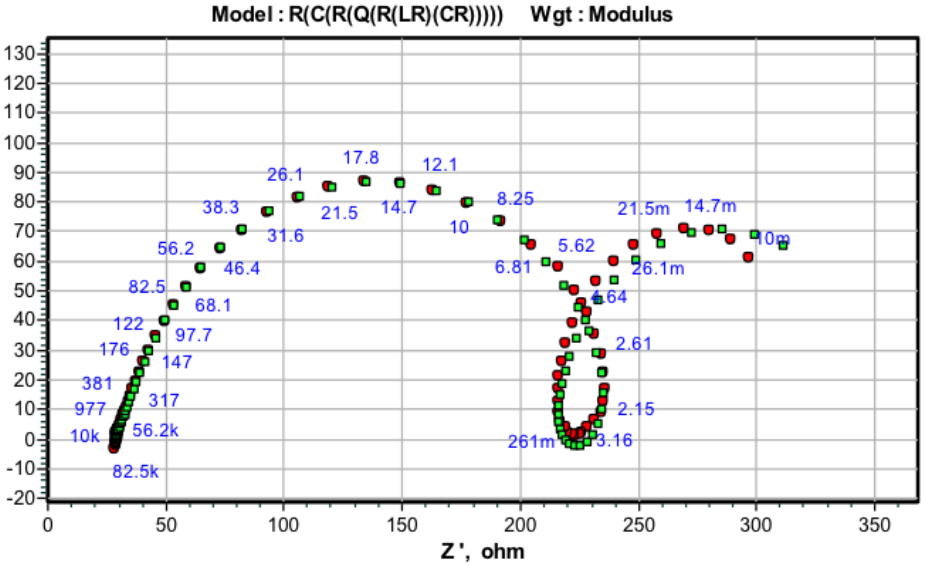

Fig. 4b: Impedance data obtained for 6061 Al-15 vol. pct. $SiC_{(P)}$ composite corrosion in 0.05M HCl at 35 °C

metal, binding of the inhibitor molecule and formation of porous layer etc [31]. The physical phenomena, surface inhomogeneous can be quantified by these parameters [32].

$$C_{dl} = Q_{dl} \times (2\pi f_{max})^{(a-1)} \quad (5)$$

Compared to nyquist plot, Bode plot analysis is simple one. Bode diagram gives a clear explanation to how the electrochemical system behaves depending upon the frequency and it also reduces the experimental data dispersion. Bode plot is most convenient for the extrapolation of the impedance data at LF and for its analysis [33].

Figure 5 discloses the bode plots obtained at OCP for 6061Al-15%$_{(v)}$SiC$_{(P)}$ without and with various concentration of inhibitor. From the figure, it was come to know that impedance value is larger in presence of inhibitor when compared with blank which indicates, decrease in the corrosion rate with the addition of inhibitor.

Figure 6 revels the plots of Bode magnitude. The plots showed only single slope for both blank and with inhibited systems, the Rp values were obtained from the difference between HF limit and LF limit in Bode plots. These differences in Bode plot became more and more with increasing the concentration of the adding inhibitor [34].

The polarization resistance (R_P) values are inversely proportional to the corrosion current density (i_{corr}). The inhibition efficiency can be calculated by using the equation (6).

$$I.E(\%) = \frac{R_{P(inh)} - R_P}{R_{P(inh)}} x\ 100 \quad (6)$$

R_P and $R_{P(inh)}$ are the polarization resistance in the absence and in the presence of the inhibitor.

As R_P value obtained from Potentiodynamic polarization measurement is in good agreement with R_P value obtained from Electrochemical Impedance Spectroscopy studies indicates that corrosion rate does not depends upon the technique used but it depends upon the behavior of the inhibitor [35, 36].

Table 3 discloses that R_P values were increased with enhancing the concentration of inhibitor but C_{dl} value decreased because of increase in the thickness of electrical double layer at M^+/solution interface [37].

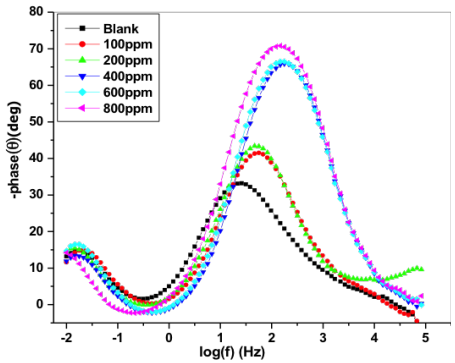

Fig. 5: Bode phase plots for the corrosion of 6061 Al-15 vol. pct. $SiC_{(P)}$ composite in 0.05M HCl at 35 °C in the presence of various concentration of inhibitors

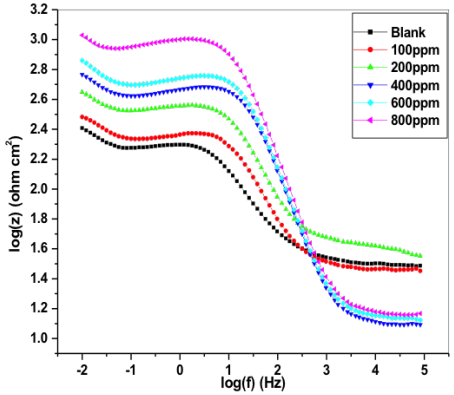

Fig. 6: Bode magnitude plots for the corrosion of 6061 Al-15 vol. pct. $SiC_{(P)}$ composite in 0.05M HCl at 35 °C in the presence of various concentration of inhibitor

3.3. Effect of temperature

It is evidence from the table 2 that, I.E(%) of the starch inhibitor increased with increase in the temperature. This increase in I.E (%) is due to the firm adsorption of the adsorbed inhibitor molecule onto the surface of the metal [38]. The activation parameters such as energy of activation (E_a), the enthalpy (ΔH_a) and entropy of activation (ΔS_a) values can be obtained by studying the effect of temperature on the adsorption of inhibitor over the surface of the metal. The energy of activation (E_a) can be calculated by the study of temperature effect on the Al-composite corrosion process in the uninhibited and the inhibited solution from Arrhenius law equation [39],

Tab. 3: Impedance values obtained for the corrosion 6061 Al-15 vol. pct. $SiC_{(P)}$ composite in 0.05 M HCl in the absence and presence of various concentrations of starch

Temp (°C)	[Starch] ppm	C_{dl} (µF cm^{-2})	R_p (Ω cm^2)	I.E(%)
30	Blank	192.65	118	---
	100	129.86	173	31.79
	200	120.49	188	37.20
	400	117.60	234	49.57
	600	115.80	248	52.40
	800	112.64	399	70.42
35	Blank	206.76	103	---
	100	129.74	156	33.97
	200	121.65	224	54.01
	400	118.09	312	66.98
	600	116.10	346	70.23
	800	112.36	498	79.31
40	Blank	227.89	73	---
	100	129.98	198	63.13
	200	120.42	253	71.14
	400	117.93	282	74.46
	600	116.62	333	78.07
	800	113.80	638	88.55
45	Blank	267.90	51	---
	100	130.65	166	69.27
	200	121.53	230	77.82
	400	119.87	357	85.71
	600	118.09	372	86.29
	800	112.59	408	87.50
50	Blank	281.65	46	---
	100	129.98	165	72.12
	200	121.65	310	85.16
	400	119.43	356	87.07
	600	118.93	546	91.57
	800	113.69	598	92.30

$$\ln (CR) = B - \frac{E_a}{RT} \quad (7)$$

where, B is Arrhenius constant which depends upon the metal type and R is equal to 8.314 JK^{-1}mol^{-1} (universal gas constant), T is the absolute temperature. Figure 7 is the Arrhenius plot for the Al-composite material. The plots of ln (CR) verses 1/T gave collinear lines with a slope corresponding to $-E_a/R$ from which energy of activation (E_a) values can be obtained for the Al-composite corrosion and its inhibition process.

The transition state equation was used to calculate the enthalpy (ΔH_a) and entropy of activation (ΔS_a) for the dissolution of metal. The transition state equation is [40],

$$CR = \frac{RT}{Nh}\exp\left(\frac{\Delta S_a}{R}\right)\exp\left(\frac{\Delta H_a}{RT}\right) \quad (8)$$

Where h is planks constant (6.626×10^{-34} J s), N is Avogadro's number (6.023×10^{23} mol^{-1}). The plot of ln (CR/T) verses 1/T gave a collinear line with slope corresponding to $-(\Delta H_a)/R$, which gave the value of enthalpy of activation and the intercept corresponding to ln(R/Nh) + $\Delta S_a/R$ gave the value of entropy of activation. Figure 8 is the plot of ln (CR/T) verses 1/T for Al-composite in various concentration of starch inhibitor in 0.05M hydrochloric acid. Activation parameters for the corrosion of Al-composite in 0.05M hydrochloric acid containing different concentrations of starch inhibitors are tabulated in table 4.

Energy of activation (E_a) values of the inhibited solutions is lesser when compared with that of uninhibited solution. This decrease in the E_a value of the inhibited solution is suggestive of chemical adsorption of the starch inhibitor on the surface of the metal with a resultant closer approach to equilibrium during the experiment at higher temperatures [41, 42]. The adsorbed molecule on the metal surface blocks the process of charge transfer during the corrosion of Al-composite, this leads to the decrease in energy of activation. In the other words, the inhibitor molecule gets chemically adsorbed on the metal surface and reduces the electrochemical corrosion process [43 – 45]. The positive signs of ΔH_a reflects the endothermic process of Al-composite metal dissolution process [46].

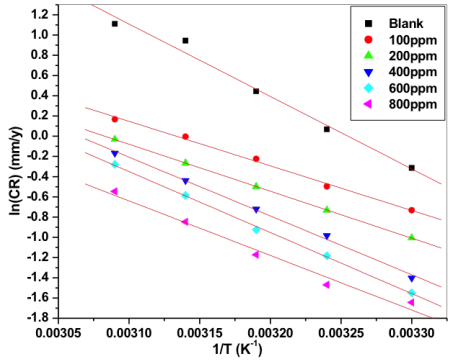

Fig.7: Plots of ln(CR) verses 1/T for corrosion inhibition of 6061 Al-15 vol. pct. $SiC_{(P)}$ composite in 0.05M HCl containing different concentration of inhibitors

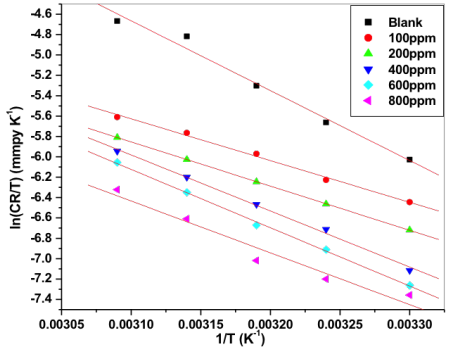

Fig. 8: Plots of ln(CR/T) vs 1/T for the corrosion of 6061 Al-15 vol. pct. SiC(P) composite in 0.05M HCl containing different concentration of inhibitors

The entropy of activation (ΔS_a) values are negative which indicates that, in rate determining step the activated complex is association not dissociation i.e., decrease in the disorderness on going from reactants towards the activated complex [47, 48].

3.4 Adsorption isotherm

The mechanism of inhibition of corrosion by the addition of starch can be understood by studying the adsorption behavior of inhibitor molecule on 6061 Al-15 vol. pct. $SiC_{(P)}$ composite metal surface. Information regarding how the inhibitor molecule interacted with 6061 Al-15 vol. pct. $SiC_{(P)}$ composite surface can be obtained by adsorption isotherm. (θ) Degree of surface coverage values for different concentration was obtained from Potentiodynamic polarization studies and it was applied to various adsorption isotherms such as Langmuir, Freundlich, Temkin and Frumkin. The data was best

Tab. 4: Activation parameters for the corrosion of 6061 Al-15 vol. pct. $SiC_{(P)}$ composite in 0.05M HCl containing different concentrations of inhibitor

[Starch] g L^{-1}	E_a (kJ mol^{-1})	ΔH_a (kJ mol^{-1})	ΔS_a (J mol^{-1} K^{-1})
Blank	59.53	56.98	−180.95
0.2	36.62	34.07	−190.45
0.4	38.61	36.06	−189.94
0.6	48.30	45.75	−186.45
0.8	50.14	47.59	−185.91
1.0	44.87	42.26	−188.21

fitted with Langmuir adsorption isotherm which can be related by the relationship (9) [47]

$$\frac{C}{\theta} = \frac{1}{K} + C \quad (9)$$

Where, K is adsorption/desorption equilibrium constant ($Lmol^{-1}$), C is the concentration of inhibitor molecule in the electrolyte, then θ is given by the equation (10)

$$\theta = \frac{I.E\ (\%)}{100} \quad (10)$$

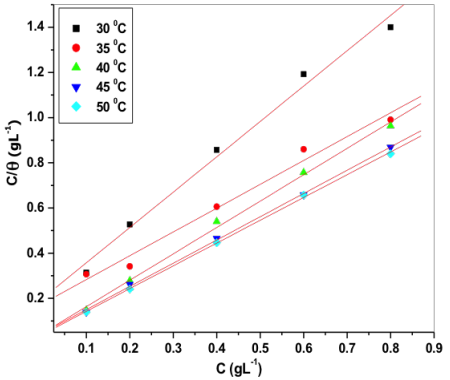

Fig. 9: Langmuir adsorption isotherm for the adsorption of starch on 6061 Al-15 vol. pct. $SiC_{(P)}$ composite in 0.05M HCl at different temperature

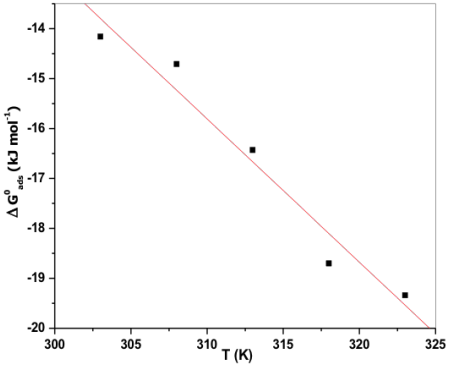

Fig. 10: ΔG^0_{ads} vs T plot

The plot of $\frac{C}{\theta}$ verses C gave straight line; from the intercept $\frac{1}{K}$ values were obtained. Figure 9 indicates Langmuir adsorption isotherm plot for 6061 Al-15 vol. pct. $SiC_{(P)}$ composite material.

The deviation from the unity value in the adsorption isotherm slope may due to the interaction between the adsorbed inhibitor molecule and Al–composite metal surface. The assumption of Langmuir adsorption isotherm is, adsorbed inhibitor molecule will not interact with each other; but this assumption not obeys in case of organic substances containing polar groups, which blocks anodic and cathodic sites of metal surface. Standard free energy of adsorption (ΔG^0_{ads}) can be calculated by using the values of K, which is related by the equation (11),

$$K = \frac{1}{55.55}\ \exp\left(\frac{\Delta G^0_{ads}}{RT}\right) \quad (11)$$

where R is universal gas constant, T is the absolute temperature; the value 55.55 in the above equation is the concentration of water in the solution in mol^{-1}.

Standard enthalpy of adsorption (ΔH^0_{ads}) and Standard entropy of adsorption (ΔS^0_{ads}) values were obtained by plotting ΔG^0_{ads} verses T. Figure 10 shows the plot of ΔG^0_{ads} verses T, which gives linear plot; from the slope ΔS^0_{ads} value and from the intercept ΔH^0_{ads} values were calculated by using Gibbs Helmholtz equation (12).

$$\Delta G^0_{ads} = \Delta H^0_{ads} - T\Delta S^0_{ads} \quad (12)$$

According to Bentiss F et al, if ΔG^0_{ads} value is up to –20kJmol^{-1} then it is considered that there is an electrostatic interaction between the protonated inhibitor species and negatively charged metal surface i.e. physisorption. More negative value than –40kJmol^{-1} indicates sharing or transfer electrons from the inhibitor molecule to the surface of the metal through coordinate bond

Tab. 5: Thermodynamic parameters for the corrosion of 6061 Al-15 vol. pct. $SiC_{(P)}$ composite in 0.05M HCl

Temp (K)	ΔG^0_{ads} (kJ mol^{-1})	ΔH^0_{ads} (kJ mol^{-1})	ΔS^0_{ads} (J mol^{-1}K^{-1})
303	–14.16		
308	–14.71	73.16	– 287
313	–16.43		
318	–18.70		
323	–19.34		

formation i.e. chemisorption [48]. Here, the negative value implies feasibility in corrosion process and the spontaneous adsorption of the inhibitor molecule on the metal surface. The ΔG^0_{ads} value is less than –20kJmol^{-1} and its value increased with increase in the temperature, this indicates the adsorption of the inhibitor molecule on 6061 Al-15 vol. pct. $SiC_{(P)}$ composite is predominantly chemical adsorption [49].

If ΔH^0_{ads} value less than –40kJmol^{-1} then it correspond to physical adsorption, if it is approaching 100kJmol^{-1}, then it is considered as chemical adsorption. In this case ΔH^0_{ads} value is positive and it is approaching 100kJmol^{-1} i.e. ΔH^0_{ads} =73.16 kJmol^{-1}, this indicates the chemical adsorption of inhibitor molecule over the surface of the Al–composite metal. The negative value of ΔS^0_{ads} is due to decrease in the disorderness of adsorbed inhibitor species.

3.5 Mechanism of corrosion

3.5.1 Anodic dissolution reaction

In 0.05M HCl, the protective layer of aluminum gets destroyed and corrosion attack takes place. But corrosion rate of Al–composite is high due to the reinforcement of SiC particulates. Due to more negative potential of aluminum in galvanic series (E = –1.66V) following reaction takes place (Eq. 13),

$$Al \rightarrow Al^{3+} + 2e^- \quad (13)$$

The chloride ions enhances the rate of metal dissolution, as they are chemically bonded in the interface it leads to the formation of mixture of oxohydroxo and chloro complexes of different forms given below [50]

$$Al\,[\,O_x(OH)_y(H_2O)_z\,] + Cl^- \rightarrow Al\,[O_x(OH)_{y-1}\,Cl\,(H_2O)_z\,] + OH^- \quad (14)$$

$$(AlOOH)_4.\,H_2O + Cl^- \rightarrow (AlOOH)_3.\,AlOCl.\,H_2O + OH^- \quad (15)$$

$$AlOOH + Cl^- \rightarrow AlOCl + OH^- \quad (16)$$

$$Al(OH)_3 + Cl^- \rightarrow Al\,(OH)_2\,Cl + OH^- \quad (17)$$

Then, $[Al(Cl)_6]^{-3}$ is formed. Starch inhibitors containing plenty of –OH groups (shown in fig. 11) get interacts with metal and protects the metal from undergoing corrosion.

$$[Al(Cl)_6]^{3-}{}_{ads} + [Starch]^+ \rightarrow [AlCl_6]^{3-}[Starch]^+ \leftrightarrows [Al\ Starch]^{3+}{}_{ads} + Cl_6^- \quad (18)$$

3.5.2 Hydrogen evolution reaction

General cathodic reduction reaction in acidic environment is given below,

$$Al_2O_3 + H_3O^+ + e^- \leftrightarrows Al_2O_3\,(H_2O) + 1/2H_2 \quad (19)$$

The large polymer starch competes with protons and occupy cathodic region, forming Al–starch (Eq. 20). The proton size is negligible compared to large molecular weight compound polymer starch. Therefore Starch as it is larger molecule; it

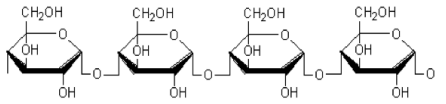

Fig. 11(a): Structure of amylose

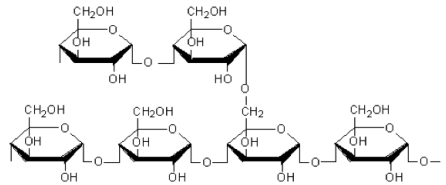

Fig. 11(b): Structure of amylopectin

covers almost all the parts of the metal and brings down both cathodic and anodic reactions under control.

$$Al + [Starch] + e^{-} \leftrightarrows [Al{-}starch]_{ads} \quad (20)$$

The presence of π–electrons and lone pair of electrons on oxygen atom are involved in protecting Al surface undergoing corrosion. The electrons are donated to the vacant p–orbitals of Al which leads to the formation of co–ordinate bond between the metal surface and inhibitor molecule, as the metal get protected by forming co–ordinate bond with inhibitor molecule, it can be suggest the chemical adsorption of the inhibitor molecule.

3.6 Surface studies

3.6.1 SEM and elemental analysis

The SEM image of freshly polished 6061 Al-15 vol. pct. $SiC_{(P)}$ composite material is shown in the Figure 12(a), this image shows smooth surface of the metal with reinforced nanostructured SiC particulates. SEM image of the sample in contact with 0.05 M hydrochloric acid is shown in Figure 12(b). When the Surface of 6061 Al-15 vol. pct. $SiC_{(P)}$ composite material was observed in higher magnification its surface seems to be rough due to the formation of pits and intergranular. Here, 6061 Al-15 vol. pct. $SiC_{(P)}$ composite is highly susceptible to intergranular corrosion. This is either may be due to the presence of SiC particulates (present along the grain boundaries) which acts as anodic to aluminum alloy or due to the depleted zones of copper present adjacent to grain boundaries in copper-containing alloys [51]. It is evident that, after the addition of inhibitor the surface has become smooth. Figure 12(c) shows the smooth surface of 6061 Al-15 vol. pct. $SiC_{(P)}$ composite. This is mainly because of the formation of inhibitor film on the surface of the metal.

Tab. 6: EDX data obtained for 6061 Al-15 vol. pct. $SiC_{(P)}$ composite surface analysis

Samples	(%) Composition				
	Al	Si	O	Cl	C
Freshly polished 6061 Al-15 vol. pct. $SiC_{(P)}$ composite	79.19	13.88	6.93	---	24.48
Specimen immersed in 0.05 M HCl medium	53.24	6.32	21.30	0.17	19.13
Specimen + 0.05M HCl + 800ppm starch	54.18	10.65	10.68	---	26.64

Tab. 7: AFM data obtained for 6061 Al-15 vol. pct. $SiC_{(P)}$ composite surface analysis

Samples	R_a (nm)	R_q (nm)	(P-V) (nm)
Freshly polished 6061 Al-15 vol. pct. $SiC_{(P)}$ composite	52.6	68.3	1513
Specimen immersed in 0.05 M HCl medium	78.9	146	2522
Specimen + 0.05M HCl + 800ppm starch	35.7	47.6	640

EDX studies were carried to un-corroded, corroded and inhibited samples. Freshly polished sample showed the peak for aluminum, reinforced SiC and for oxygen; these suggest the presence of reinforced SiC particulates and aluminum oxide/ hydroxide. Extra peak for chloride in corroded sample is due to the formation of aluminum chloride after corrosion. Peak of carbon is observed for un-corroded, corroded and inhibited samples, this is due to the presence of SiC, which is also supported from the table 6 indicating the (%) composition for carbon, but (%) composition for carbon in inhibited solution is more when compared to uninhibited solution, indicating the formation of protective inhibitor layer over the surface of the metal.

3.6.2. AFM analysis

The 3-dimensional (3D) images of 6061 Al-15 vol. pct. $SiC_{(P)}$ composite is given in the figure 13. Freshly polished metal surface image, specimen immersed in 0.05 M HCl medium and specimen + 0.05M HCl + 800ppm starch is given in the figure 13(a), 13(b) & 13(c) respectively. The average surface roughness (R_a), Root mean square (RMS) roughness (R_q) and peak-valley maximum (P-V) values were given in the table 7.

It is evident from the table 7, that R_a, R_q and (P-V) values of inhibited sample is very less compared to polished and uninhibited sample this indicates the adsorption of the inhibitor molecule over the metal surface.

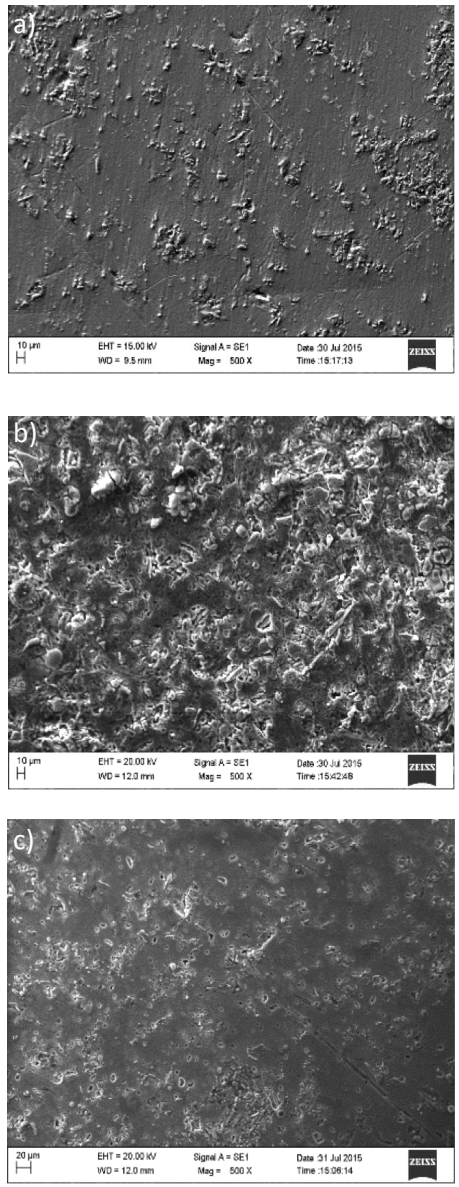

Fig. 12: SEM image of 6061 Al-15 vol. pct. $SiC_{(P)}$ composite material of a) freshly polished surface, b) immersed in 0.05 M HCl medium, c) immersed in 0.05 M HCl medium + 800ppm starch at 30°C

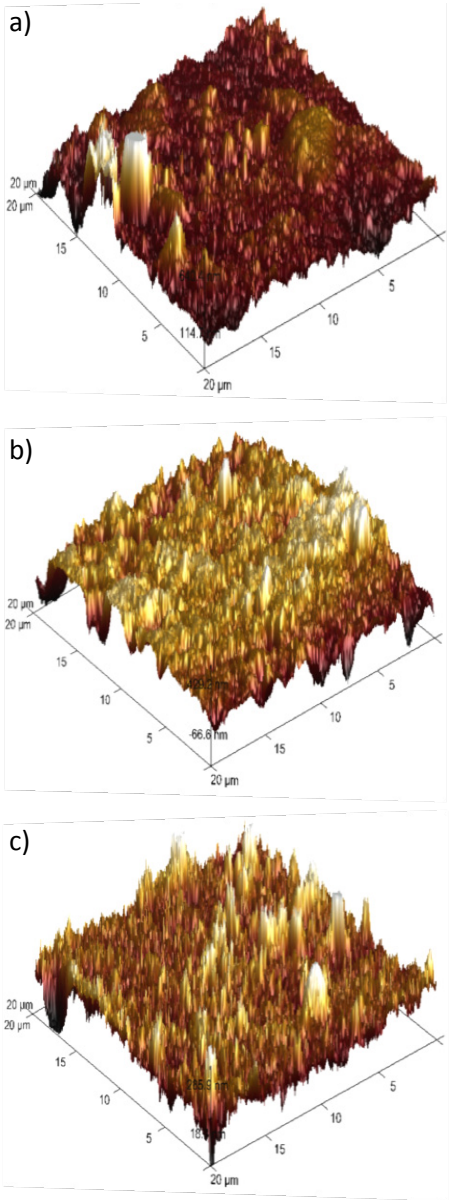

Fig. 13: 3D image of 6061 Al-15 vol. pct. $SiC_{(P)}$ composite material of a) freshly polished surface, b) immersed in 0.05 M HCl medium, c) immersed in 0.05 M HCl medium + 800ppm starch at 30°C

3.6.3 XRD Analysis

XRD spectrums for the corroded powdered sample and for the sample with inhibitor were given in the figure 14(a) and 14(b) respectively.

The figure 14(a) showed that intensity of the peak is more i.e. 147.54, 265.55, 986.52, 9760.95, 196.46, 3926.88, 399.15, 1901.55, 308.32, and 1488.2; figure 14(b) showed less intense peak i.e. 136.77, 237.28, 784.94, 9069.98, 139.23, 3867.45, 326.62, 1781.61 and 1383.39. This decrease in the peak intensity for the sample with inhibitor is due to the adsorption of the starch molecule onto the surface of the metal.

Conclusion

Based upon the studies carried to control the corrosion 6061 Al-15 vol. pct. $SiC_{(P)}$ composite material in 0.05M HCl following conclusions are drawn,

a. Starch acted as a mixed inhibitor by controlling both dissolution of metal ion and hydrogen gas evolution reaction.
b. I.E. (%) of starch increased with increase in the [starch] and as well as temperature.
c. Adsorption, kinetic and thermodynamic studies on corrosion control of Al-composite using starch inhibitor at lower acid concentration showed chemical adsorption followed by Langmuir adsorption isotherm.
d. Surface studies such as SEM, EDAX, AFM & XRD supported for the adsorption of starch molecule onto the surface of the metal.

Acknowledgement

Ms Charitha B. P. is greatful to Manipal University for Research Fellowship and Department of Chemistry M.I.T. Manipal for laboratory facilities.

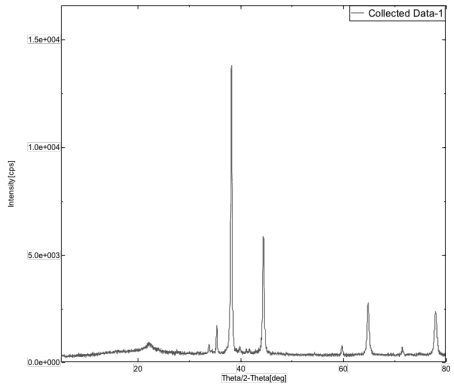

Fig. 14(a): XRD spectrum for corroded 6061 Al-15 vol. pct. $SiC_{(P)}$ composite

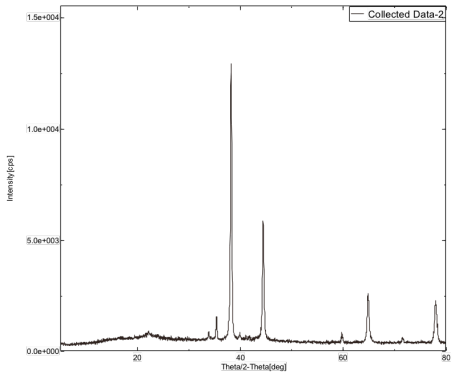

Fig. 14(b): XRD spectrum for 6061 Al-15 vol. pct. $SiC_{(P)}$ composite immersed in inhibited solution

References

[1] B. Bobic., S. Mitrovic, M. Babic, I. Bobic, "Corrosion of Metal-Matrix Composites with Aluminium Alloy Substrate", McGraw-Hill, New York,(2010).
[2] T.H. Sanders Jr., E.A. Starke Jr., "Proceedings of the Fifth International Conference on Al–Lithium alloys," Materials & Composites Engineering Publications Ltd., Birmingham, UK, (1989), 1.
[3] C. Monticelli, F. Zucchi, G. Brunoro, G. Trabanelli, "Corrosion and corrosion inhibition of alumina particulate/aluminium alloys metal matrix composites in neutral chloride solutions," J. Appl. Electrochem, 27 (1997) 325.
[4] A. Pardo, M.C. Merino, S. Merino, F. Viejo, M. Carboneras, R. Arrabal, "Influence of reinforcement proportion and matrix composition on pitting corrosion behaviour of cast aluminium matrix composites (A3xx.x/SiCp," Corros. Sci. 47 (2005) 1750.
[5] C.E. Da Costa, F. Velasco, J.M. Toralba Rev. Metal. Madrid, "Metal Matrix Composites: Part I—Properties and Applications," 36 (2000) 179.
[6] P.K. Rohatgi, " Cast Aluminum-Matrix Composites for Automotive Applications (Featured Overview)," JOM 43 (1991) 10.
[7] A. Pardo, M.C. Merino, S. Merino, M.D. Lopez, F. Viejo, M. Carboneras, " Improvement of Corrosion Behavior of A3xxx/SiCP in 3.5 N NaCl Solution," Mater. Corros. 54 (2003) 311.
[8] C.J. Peel, R. Moreton, P.J. Gregson, E.P. Hunt, "Proceedings of the XIII International Conference on Society of Advanced Material and Process Engineering," SAMPE, Covina, CA, (1991) 189.
[9] M. N. Desai, S.S. Rana, M.H. Gandhi, Corrosion inhibitors for aluminium in hydrochloric acid- Aliphatic polyamines for aluminium 57S, Anticorrosion, Methods & Mater. 19(3) (1972) 16-19.
[10] T. L. Rama Char, O. K. Padma, Trans. Inst. Chern. Engnrs. 47 (1969) 177.
[11] I. N. Putilova, S. A. Balezin, B. Arannik, Metallic Corrosion Inhibitors, Pergamon, Oxford, (1960) 67.
[12] US congress, office of technology assortment, Biopolymers: making materials nature's way, (1993)
[13] Deepa prabhu, Padmalatha Rao, "Coriandrum sativum L.–A novel green inhibitor for the corrosion inhibition of aluminum in 1M phosphoric acid solution," Journal of environmental chemical engineering, 1(2013) 676–683
[14] Deepa prabhu, Padmalatha Rao, "Studies of corrosion of aluminum and 6063 aluminum alloy in phosphoric acid medium." International journal of Chem Tech research, 5 (2013), 2690–2705
[15] Deepa prabhu, Padmalatha Rao, "Garcinia indica as an environmentally safe corrosion inhibitors for aluminum in 0.5M phosphoric acid," Hindawi publishing corporation, International Journal of corrosion, (2013), 1–11
[16] E. Stupnise k-Lisac, A. Gazivoda, M. Madza rac, "Evaluation of non-toxic corrosion inhibitors for copper in sulphuric acid" Electrochim Acta, 47 (2002), 4189–4194
[17] M. Shahin, S. Bilgic, H. Yilmaz, "The inhibition effects of some cyclic nitrogen compounds on the corrosion of the steel in NaCl medium." Appl. Surf. Sci. 195 (2003) 1–7.
[18] Li, W., He, Q., S. Zhang, C. Pei, B. Hou, "Some new triazole derivatives as inhibitors for mild steel corrosion in acidic medium" J. Appl. Electrochem. 38 (2008) 289–295.
[19] M. G. Fontana, Corrosion engineering, (1987) McGraw-hill, Singapore, 3
[20] H. J. W. Lenderink, M. V. D. Linden, J.H.W. De Wit, "Corrosion of aluminum in acidic and neutral solutions," Electrochim. Acta, 38 (1993) 1989–1992.
[21] H. De Wit, H. J.W. Lenderink, "Electrochemical impendence spectroscopy as a tool to obtain mechanistic information on the passive behavior of commercial sample of aluminium," J. Electrochem.Acta., 41 (1996) 1111-1119.

[22] M. Metikos-Hukovic, R. Babic, Z. Grubac, "Corrosion protection of aluminium in acidic chloride solutions with nontoxic inhibitors," J. Appl. Electrochem. 28 (1998) 433–439.

[23] C. M. A. Brett, "Electrochemical impendence spectroscopy applied to study of aluminum corrosion", J. of Appl. Electro-chem., 20 (1990) 1000.

[24] E. J. Lee, S. I. Pyun, "The effect of oxide chemistry on the passivity of aluminium surfaces," Corros. Sci. 37 (1995) 157–168.

[25] C. M. A. Brett, "Electrochemical behavior of aluminum in basic chloride solution", J. Corros. sci., 33 (2) (1992) 203- 210.

[26] K. F. Khaled, M.M Al-Qahtani, "The inhibitive effect of some tetrazole derivatives towards Al corrosion in acid solution: Chemical, electrochemical and theoretical studies" Mater. Chem. Phys. 113 (2009) 150–158.

[27] A. Ehteram Noor "Evaluation of inhibitive action of some quaternary N-heterocyclic compounds on the corrosion of Al–Cu alloy in hydrochloric acid Mater. Chem. Phys. 114 (2009) 533–541.

[28] A. Aytac, U. Ozmen, M. Kabasakaloglu, "Investigation of some Schiff bases as acidic corrosion of alloy AA3102," Mater. Chem. Phys. 89 (2005) 176–181.

[29] M.M Frers, C. Stefenel, Mayer, T. Chierchie, "AC-Impedance measurements on aluminium in chloride containing solutions and below the pitting potential." J. Appl. Electrochem. 20 (1990) 996–999

[30] F. Mansfeld, S. Lin, K. Kim, H. Shih, "Pitting and Surface Modification of SiC/Al", J. of Corros. Sci., 27 (1987) 997.

[31] F. Mansfeld, S. Lin, S. Kim, H. Shih, "Electrochemical Impedance Spectroscopy as a Monitoring Tool for Passivation and Localized Corrosion of Al Alloys" Werkstoffe und Korrosion 39 (1988) 487.

[32] S. A. Umoren, I. B. Obot, E. E. Ebenso, P. C. Okafor, "Gum arabic as a potential corrosion inhibitor for aluminium in alkaline medium and its adsorption characteristics." Anti-Corros. Meth. Mater. 53 (2006) 277–282.

[33] L. M. Rivera-Grau et al, "Effects of organic corrosion inhibitors on the corrosion performance of 1018 carbon steel in 3% NaCl solution," Int. J. Electrochem. Sci., 8 (2013) 2491–2503

[34] G. M. Pinto, J. Nayak, A. Nityananda Shetty, "Corrosion inhibition of 6061 Al-15 vol. pct. SiC(p) composite and its base alloy in a mixture of sulphuric acid and hydrochloric acid by 4-(N,N-dimethyl amino) benzaldehyde thiosemicarbazone," Mater. Chem. Phys. 125 (2011) 628–640

[35] B. S. Sanat kumar, J. Nayak, A. N. Shetty, "The corrosion inhibition of maraging steel under weld aged condition by 1(2E)-1-(4-aminophenyl)-3-(2-thienyl)- prop-2-en-1-one in 1.5 M hydrochloric acid medium," J. Coat. Technol. Res. 4 (2011) 483–493.

[36] A. M. Abdel-Gaber, B. A. Abd-El-Nabey, I. M. Sidahmed, A. M. El-Zayady, M. Saadawy, "Inhibitive action of some plant extracts on the corrosion of steel in acidic media," Corros. Sci. 48 (2006) 2765–2779.

[37] T. Poornima, N. Jagannatha, A. Nityananda Shetty, "Studies on corrosion of annealed and aged 18 Ni 250 grade maraging steel in sulphuric acid medium," Portugal, Electrochim. Acta 28 (2010) 173–188.

[38] J. B. Bessone, D. R. Salinas, C. Mayer, M. Ebert, W. J. Lorenz, "An EIS study of aluminum barrier-type oxide films formed in different media", J. of Electrochim. Acta, (1992) 37 2283.

[39] J. Yahalom, "The significance of the energy of activation for the dissolution reaction of metal in acids," Corros. Sci. 12 (1972) 867–868.

[40] S.S. Abdel Rehim, A. M. Magdy, K. F. Ibrahim, "4-Aminoantipyrine as an inhibitor of mild steel corrosion in HCl solution," J.Appl. Electrochem. 29 (1999) 593–599.

[41] M. A. Ameer, E. Khamis, G. Al-Senani, "Effect of temperature on stability of adsorbed inhibitors on steel in phosphoric acid solution." J. Appl. Electrochem. 32 (2002) 149–156.

[42] M. M. Osman, R. A. El-Ghazawy, A. M. Al-Sabagh, "Corrosion inhibitor of some surfactants derived from maleic–oleic acid adducts on mild steel in 1 M H2SO4." Mater. Chem. Phys. 80 (2003) 55–62.

[43] E. E. Oguzie, V. O. Njoku, C. K. Enenebeaku, C. O. Akalezi, C. Obi, "Effect of hexamethylpararosaniline chloride (crystal violet) on mild steel corrosion in acidic media", J. of Corros. Sci., 50 (2008) 3481.

[44] H. Ashassi-Sorkhabi, B. Shaabani, D. Seifzadeh, "Effect of some pyrimidinic Shciff bases on the corrosion of mild steel in hydrochloric acid solution", Appl. Surf. Sci. 239 (2005) 154–164.

[45] M. Bouklah, B. Hammouti, M. Lagrenee, F. Bentiss, "Thermodynamic properties of 2,5-bis(4-methoxyphenyl)-1,3,4-oxadiazole as corrosion inhibitor for mild steel in normal sulfuric acid medium." Corros. Sci. 48, (2006) 2831–2842.

[46] M. Sahin, S. Bilgic, H. Yilmaz, "The inhibition effects of some cyclic nitrogen compounds on the corrosion of the steel in NaCl mediums" Appl. Surf. Sci., 195 (2002) 1–7.

[47] N. Soltani, M. Behpour, S. M. Ghoreishi, H. Naeimi, "Corrosion inhibition of mild steel in hydrochloric acid solution by double Schiff bases." Corros. Sci. 52 (2010) 1351–1361.

[48] F. Bentiss,, M. Traisnel, M. Lagrenee, "Influence of 2,5-bis (4- imethylaminophenyl)-1,3,4-thiadiazole on corrosion inhibition of mild steel in acidic media." J. Appl. Electrochem. 31 (2001) 41–48.

[49] M. A. Quraishi, J. Rawat, M. Ajmal, "Dithiobiurets: a novel class of acid corrosion inhibitors for mild steel." Appl. Electrochem. 30 (2000) 745–751.

[50] L. Tomesanyi, K. Varga, I. Bartik, G. Horanyi and E. Maleczki, "Electrochemical study of the pitting corrosion of aluminium and its alloys-II. Study of the interaction of chloride ions with a passive film on aluminium," Electrochimica Acta, 34(6) (1989) 855-859.

[51] www.nace.org/Corrosion-Central/Corrosion-101/Intergranular-Corrosion/

Authors

Prof. Dr. R. Padmalatha
Department of Chemistry, Manipal Institute of Technology,
Manipal University, Manipal 576104, Karnataka, India
Email: drpadmalatharao@yahoo.com

B. P. Charitha
Department of Chemistry, Manipal Institute of Technology,
Manipal University, Manipal 576104, Karnataka, India

CONTACT:

EUGEN G. LEUZE VERLAG KG
Ralf Schattmaier
Karlstraße 4
88348 Bad Saulgau
Germany

Email: ralf.schattmaier@leuze-verlag.de
Phone: +49 0 7581 4801-12
Fax: +49 0 7581 4801-10